

## NUMERICAL INVESTIGATION OF COMBINED EFFECT OF NANOFLUIDS AND MULTIPLE IMPINGING JETS ON HEAT TRANSFER

by

**Mustafa KILIC<sup>a\*</sup> and Hafiz Muhammad ALI<sup>b</sup>**

<sup>a</sup>Department of Mechanical Engineering, Adana Science and Technology University, Adana, Turkey

<sup>b</sup>Mechanical Engineering Department, King Fahd University of Petroleum and Minerals,  
Dhahran, Saudi Arabia

Original scientific paper  
<https://doi.org/10.2298/TSCI171204094K>

*The present study is focused on numerical investigation of heat enhancement and fluid-flow from a heated surface by using nanofluids with three impinging jets. Effects of different volume ratio, different heat flux and different types of nanofluids (CuO-water, Al<sub>2</sub>O<sub>3</sub>-water, Cu-water, TiO-water, and pure water) on heat transfer and fluid-flow were studied numerically. The CuO-water nanofluid was used as a coolant in the other parameter. Three impinging jets were used to cool the surface. Low Reynolds number  $k$ - $\epsilon$  turbulent model of PHONEICS CFD code was used for numerical analysis. It is obtained that increasing volume ratio from  $\phi=2\%$  to  $8\%$  causes an increase of  $10.4\%$  on average Nusselt number. Increasing heat flux six times has not a significant effect on average Nusselt number. Using Cu-water nanofluid causes an increase of  $2.2\%$ ,  $5.1\%$ ,  $4.6\%$ , and  $9.6\%$  on average Nusselt number with respect to CuO-water, TiO-water, Al<sub>2</sub>O<sub>3</sub>-water, and pure water.*

*Key words: heat transfer, nanofluid, volume ratio, impinging jet*

### Introduction

One of the optimum heat management techniques that provide high cooling efficiency in the industry is the jet impinging technique. The jet impinging technique is used to intensify heating, cooling or drying processes on a surface. The factor that makes the jet impinging technique attractive is that a high heat transfer is can be achieved on a narrow surface by means of fluid jets. Thus, at a very high rate heat transfer can be acquired with a minimum flow rate. A nanofluid is defined as a suspension of solid particles which have 1-100 nm size in a base fluid. In heat transfer applications using nanofluid, the particles suspended in the base fluid, expand thermal capacity of the fluid. Interactions and collisions between particles cause to increase in turbulence and turbulence intensity of the transition surface. Turbulence intensity and large surface area enables more heat transfer. Nanoparticles carry 20% of their atoms at the surface that makes them ready to heat transfer. Another advantage of using nanofluids is the particle agitation cause micro-convection in the fluid due to its very small size and therefore, increases the heat transfer in particular heat transfer from surfaces with high heat flux, as well as industry, medicine and space research. Many studies on nanofluids or impinging jets can be found in the literature. Kilic *et al.* [1] and Kilic [2] surveyed the cooling of a flat plate with the support of the impinging fluid air jet for different Reynolds numbers and dimensionless channel heights. The mean Nusselt number was found to

\* Corresponding author, e-mail: mkilic@adanabtu.edu.tr

increase by 49.5% in  $Re = 4000-10000$  and 17.9% in  $H/D_h = 4-10$ . Manca *et al.* [3] surveyed the effect of impinging jets on heat transfer from a flat plate with a constant heat flux when pure water and  $Al_2O_3$ -water nanofluids were used as a working fluid. Jet Reynolds number ( $Re = 100-400$ ) and dimensionless channel height ( $H/D_h = 4-10$ ) are the parameters used in operation. It has been stated that as the Reynolds number and the concentration of the particles in the fluid increases, the local heat transfer coefficient and the Nusselt number increase. The highest increase (36%) in the average heat transfer coefficient was obtained when  $H/W = 10$  and the nanoparticle volume ratios are  $\varphi = 5\%$ . Lin *et al.* [4] experimentally investigated heat transfer in confined air jets. The effects of Reynolds number and jet-target plate spacing on heat transfer were studied in this study. As a result of local and average Nusselt numbers at the stagnation point, it has been found that effect of the change in jet-target plate distance is not very important on the heat transfer, but the increase in Reynolds number increases heat transfer. Two experimental correlations were determined for mean Nusselt number and Nusselt number at the stagnation point in the range of  $190 \leq Re \leq 1537$  and  $1 \leq H/W \leq 8$ . McGuinn *et al.* [5] numerically and experimentally investigated the heat transfer of the flow from the nozzle with two separate output geometries (straight out and shaped). The jet flow is applied to a copper plate representing uniform temperature. The variation of Nusselt number for different flow frequencies and different nozzle-plate distances was investigated. Frequency variation and surface distance hydraulic diameter ratio was investigated in the range of 40-160 Hz and  $(H/D)$  1-6, respectively. As a result, it has been observed that the shaped nozzle provides more efficient heat transfer than straight nozzle. At the same time, it has been found that uniform flow from the shaped nozzle delays flow disturbances causing turbulent flow. Consequently, it was obtained that the heat transfer in the surface is not only depends on the turbulence formed but also depends on the flow geometry of the surface. Teamah *et al.* [6] investigated heat transfer and flow structure formed by  $Al_2O_3$  nanofluid to flat plate by experimentally and numerically with various Reynolds number ( $Re = 3000-32000$ ) and different volume ratio of nanofluids ( $\varphi = 0-10\%$ ). As the nanoparticles in the base fluid increases, the heat transfer from the surface increases and heat transfer coefficient can be enhanced by 62% according to the water is used base fluid only. They observed that heat transfer can be increased of 8.9% by using CuO-water with respect to  $Al_2O_3$ -water. Sun *et al.* [7] researched the effect of a single impinging jet using Cu-water nanofluids as working fluid on heat transfer. It has been determined that when the nanofluid is used, important enhancement can be achieved in heat transfer with respect to the use of water only, no significant change in pressure drop, a higher heat transfer coefficient is obtained when a circular nozzle is used, and a higher heat transfer coefficient is obtained when the jet angle is  $90^\circ$ . Umar *et al.* [8] investigated the heat transfer from constant heat flux surface in laminar flow condition using varied ratios of Cu-water nanofluid. As a result, it was found that as the particle volume ratio increased and the Reynolds number increased, the heat transfer coefficient increases, the highest increase in heat transfer coefficient (61%) occurred at a particle volume ratio of 4% and Reynolds number  $Re = 605$ . Naphon *et al.* [9] investigated the heat transfer between the nanofluids (titanium-ethanol) and the closed two-phase thermosiphon. It was found that achieving a 10.6% improvement in evaporation heat transfer coefficient in the case of using nanofluid compared to only ethanol. Kilic and Ozcan [10] investigated the heat transfer from a high heat flux surfaces for different parameters using nanofluids and multiple impinging jets. It was found that increase on Reynolds number and decrease on particle diameter causes an increase on heat transfer. The use of Cu-water nanofluid causes an increase of 9.3% and 8.4% on heat transfer according to the use of  $Al_2O_3$ -water and TiO-water nanofluid. There are some studies about investigation of characterization of nanofluids and impinging jet applications in literature. But there is not any study about investigation of effect of different nanofluids on heat transfer with multiple impinging jets. So

motivation and contribution of this study to literature to understand intricate process of combined effects of nanofluids and multiple impinging jets on heat transfer from a high heat flux surface for different volume ratio, different heat flux and different types of nanofluids. So this study is different from the studies at literature by evaluating combined effect of impinging jets and nanofluids for different parameters.

### Numerical model

Low Reynolds number  $k-\varepsilon$  turbulence model of PHOENICS CFD code was used for this numerical analysis. The CFD simulation domain is shown in fig. 1 Mesh structure is shown in fig. 2.

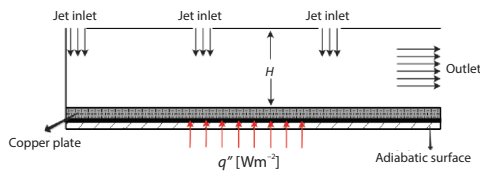


Figure 1. The CFD simulation model

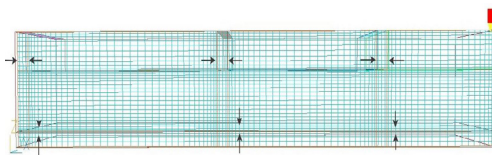


Figure 2. Mesh structure

The continuity, Reynolds averaged momentum and time averaged energy equations governing 3-D steady, flow of fluid with constant properties used for turbulent solutions can be written in the Cartesian co-ordinate system:

- continuity equation

$$\frac{\partial U_i}{\partial x_i} = 0 \quad (1)$$

- momentum equation

$$\rho U_i \frac{\partial U_j}{\partial x_i} = -\frac{\partial P}{\partial x_j} + \frac{\partial}{\partial x_i} \left[ \mu \left( \frac{\partial U_i}{\partial x_j} + \frac{\partial U_j}{\partial x_i} \right) - \overline{\rho u'_i u'_j} \right] \quad (2)$$

- energy equation

$$\rho c_p U_i \frac{\partial T}{\partial x_i} = \frac{\partial}{\partial x_i} \left[ k \frac{\partial T}{\partial x_i} - \rho c_p \overline{u'_i T'} \right] \quad (3)$$

All the boundary conditions used in the study are summarized in tab. 1. It was used  $96 \times 15 \times 34$  (48960 elements) meshes for this application. Mesh structure was prepared according to flow conditions. In order to get more precise numerical results, we intensified mesh numbers in some region as jet inlet, surface of copper plate. Sweep number was studied between 400 and 1000 and cell number was also studied between 24 and 44. It is observed that numerical geometry was independent from sweep number and cell number when sweep number was 600 and cell number was  $96 \times 15 \times 34$ . Variation of  $T_{avg}$  for different sweep number and grid number was shown in figs. 3 and 4.

Table 1. Boundary conditions

	$U$ [ $\text{ms}^{-1}$ ]	$V$ [ $\text{ms}^{-1}$ ]	$W$ [ $\text{ms}^{-1}$ ]	$T$ [ $^{\circ}\text{C}$ ]	$k$	$\varepsilon$
$W_{\text{jet,inlet}} (W_1, W_2, W_3)$	$U = 0$	$V = 0$	$W = W_{\text{inlet}}$	$T = T_{\text{inlet}}$	$T_i W_{\text{jet}}$	$(C_\mu C_d)^{3/4} (k^{3/2}/L)$
Cu plate	$U = 0$	$V = 0$	$W = 0$	$q = q_{\text{outlet}}$	$k = 0$	$\partial \varepsilon / \partial z = 0$
Outlet	$\partial U / \partial x = 0$	$\partial V / \partial x = 0$	$\partial W / \partial x = 0$	$T = T_{\text{out}}$	$\partial k / \partial x = 0$	$\partial \varepsilon / \partial x = 0$
Front and back wall	$U = 0$	$V = 0$	$W = 0$	$\partial T / \partial y = 0$	–	–
Top wall	$U = 0$	$V = 0$	$W = 0$	$\partial U / \partial z = 0$	–	–

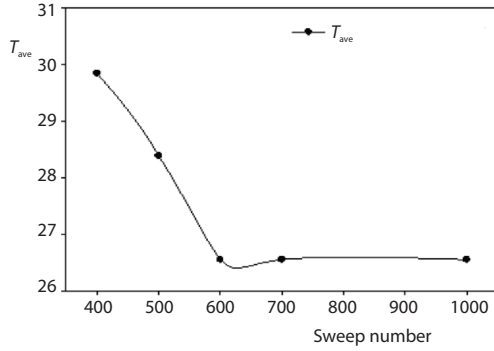


Figure 3. Variation of  $T_{avg}$  for different sweep number

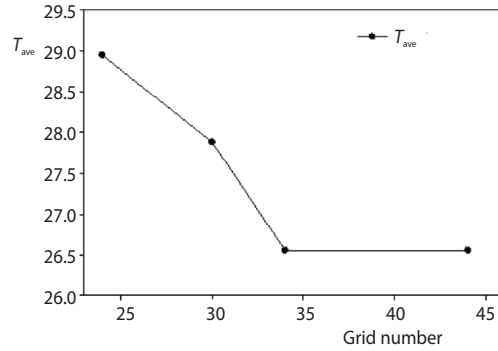


Figure 4. Variation of  $T_{avg}$  for different grid number

Numerical results were verified with the experimental results of Li *et al.* [11] and correlation of Xuan and Li [12]. Verification of numerical model is shown in fig. 5.

Difference between numerical results and experimental results is less than 15% for  $Re = 8000$  and 5% for  $Re = 12000$ . It is determined that Brownian motion effect is more significant for low Reynolds number. For this numerical model nanofluids are assumed one phase. So difference between numerical results and experimental results is decreasing while increasing Reynolds number. Reynolds number for this application is 36200. So it can be obtained that difference between numerical results and experimental results is less than 5% for this study. Comparison of low Reynolds number  $k-\epsilon$  turbulence model with other turbulence models (standard  $k-\epsilon$  model,  $k-\omega$  model) was shown in fig. 6. It is obtained that difference between numerical results and experimental results is less for low Reynolds number  $k-\epsilon$  turbulence model with respect to other turbulence models. So low Reynolds number  $k-\epsilon$  turbulence model represents fluid-flow and heat transfer more correctly than other turbulence models.

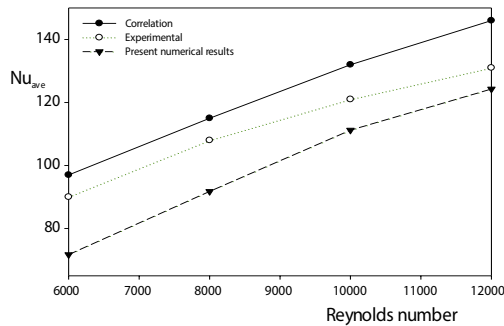


Figure 5. Verification of model with experimental results and correlations

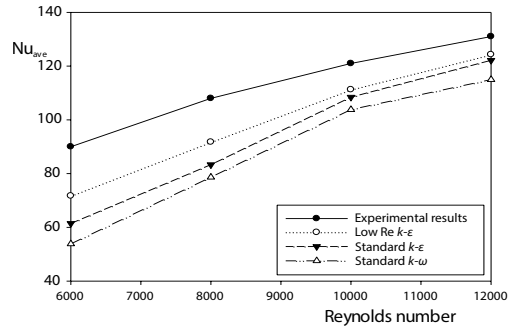


Figure 6. Comparison of low Reynolds number  $k-\epsilon$  turbulence model with experimental results and other turbulence models

Data reduction

The heat transfer from the surface will take place by convection, conduction and radiation:

$$Q_{convection} = Q_{total} - Q_{conduction} - Q_{radiation} \tag{4}$$

Heat generated by the heater placed under the copper plate will be transmitted to the upper surface of the plate through the copper plate thickness by conduction, and as a result, the

plate surface will be cooled by using nanofluid with impinging jet. Heat transfer by conduction along the plate:

$$Q_{\text{conduction}} = \frac{-k_c A_c (T_{\text{bottom}} - T_{\text{upper}})}{L_c} \quad (5)$$

where  $k_c$  is the heat transfer coefficient of the copper plate,  $A_c$  – the copper plate surface area, and  $L_c$  – the copper plate thickness. It is assumed that heat transfer with radiation is negligible in this study because surface temperature is under 573.15 K.

Heat transfer from surface with convection:

$$Q_{\text{convection}} = hA\Delta T \quad (6)$$

where  $h$  is the heat transfer coefficient,  $A$  – the convection surface area, and  $\Delta T$  ( $\Delta T = T_s - T_{\text{bulk}}$ ) – the difference between the measured surface temperature and the fluid mean temperature. Nusselt number is the dimensionless parameter indicating the ratio of heat transfer with convection heat transfer with conduction. Average Nusselt number can be presented:

$$\text{Nu} = \frac{(Q_{\text{convection}} D_h)}{(T_s - T_{\text{jet}}) k_{\text{nf}}} \quad (7)$$

where  $T_s$  is the measured surface temperature,  $D_h$  – the hydraulic diameter, and  $k_{\text{nf}}$  – the coefficient of thermal conductivity of the nanofluid. Average Nusselt number can be presented as ratio of average heat transfer coefficient times characteristic length,  $D_h$ , to the coefficient of thermal conductivity of the nanofluid:

$$\text{Nu}_{\text{avg}} = \frac{h_{\text{avg}} D_h}{k_{\text{nf}}} \quad (8)$$

where  $h_{\text{avg}}$  is the average heat transfer coefficient, measured,  $D_h$  – the hydraulic diameter, and  $k_{\text{nf}}$  – the coefficient of thermal conductivity of the nanofluid. Reynolds number is used to determine for forced convection whether the flow is laminar or turbulent. Reynolds number based on turbulent flow:

$$\text{Re} = \frac{\rho_{\text{nf}} V_{\text{jet}} D_h}{\mu_{\text{nf}}} \quad (9)$$

where  $\rho_{\text{nf}}$  is the nanofluid density,  $V_{\text{jet}}$  – the jet velocity, and  $\mu_{\text{nf}}$  – the nanofluid dynamic viscosity.

The density of nanofluids is:

$$\rho_{\text{nf}} = (1 - \varphi) \rho_{\text{bf}} + \varphi \rho_p \quad (10)$$

where  $\rho_{\text{bf}}$  is the base fluid (water) density,  $\varphi$  – the volumetric ratio of the nanofluid, and  $\rho_p$  – the density of the solid particles in the nanofluid. The volumetric ratio of nanoparticles is:

$$\varphi = \frac{1}{\frac{1}{\omega} (\rho_p - \rho_{\text{bf}})} \quad (11)$$

where  $\omega$  is the density difference between the fluid and the main fluid (water). The nanofluid specific heat is calculated from:

$$C_{p_{\text{nf}}} = \frac{\varphi (\rho C_p)_p + (1 - \varphi) (\rho C_p)_f}{\rho_{\text{nf}}} \quad (12)$$

where  $C_{p(p)}$  is specific heat of particle,  $C_{p(f)}$  – specific heat of base fluid. The effective thermal conductivity of nanofluid is calculated according to Corcione [13];

$$\frac{k_{eff}}{k_f} = 1 + 4.4 \text{Re}^{0.4} \text{Pr}^{0.66} \left( \frac{T_{nf}}{T_{fr}} \right)^{10} \left( \frac{k_p}{k_f} \right)^{0.03} \varphi^{0.66} \quad (13)$$

where Re is the nanoparticle Reynolds number, Pr – the Prandtl number of the base liquid,  $k_p$  – the nanoparticle thermal conductivity,  $\varphi$  – the volume ratio of the suspended nanoparticles,  $T_{nf}$  [°K] – the nanofluid temperature, and  $T_{fr}$  – the freezing point of the base liquid.

Nanoparticle Reynolds number is defined as:

$$\text{Re} = \frac{2\rho_f k_b T}{\pi \mu f^2 d_p} \quad (14)$$

where  $k_b$  is the Boltzmann's constant. The effective dynamic viscosity of nanofluids defined as:

$$\mu_{nf} = \mu_{bf} (1 + 2.5 \varphi + 4.698 \varphi^2) \quad (15)$$

## Results and discussions

In this section, numerical results were prepared for three parameters. Effects of CuO-water nanofluid with 25 nm particle diameter for different volume ratios on heat transfer ( $\varphi = 2\%$ , 4%, 6%, and 8%). Effects of different heat flux of copper plate on heat transfer with CuO-water nanofluid ( $q'' = 37037 \text{ W/m}^2$ , 74074  $\text{W/m}^2$ , 148148  $\text{W/m}^2$ , and 222222  $\text{W/m}^2$ ). Effects of different nanofluids on heat transfer with 2% volume ratio (CuO-water,  $\text{Al}_2\text{O}_3$ -water, Cu-water, TiO-water and pure water).

### Effects of different volume ratio of CuO nanofluid

Figure 7 shows temperature of heated surface for different volume ratios ( $\varphi = 2\%$ , 4%, 6%, and 8%) of CuO-water nanofluid. Increasing volume ratio can cause precipitation and prevention of fluid-flow. For this reason volume ratio of 2% was chosen at some studies in literature. For impinging jet applications, fluid velocity is higher than channel flow. So it can be assumed that pressure drop will be less for impinging jet application. By the way, to understand effect of volume ratio on heat transfer, volume ratio was increased from  $\varphi = 2$ -8%.

It can be seen that the surface temperature decreases on stagnation point of first impinging jet. There is a temperature increase before the stagnation point of second jet. The reason of this is decreasing of the fluid velocity with effects of second jet. So location of stagnation point of second jet goes upward. When velocity of the fluid decreases, thermal boundary-layer thickness increases again. Figure 8 shows velocity vectors of CuO-water nanofluid for  $\varphi = 2\%$  and 8%, respectively.

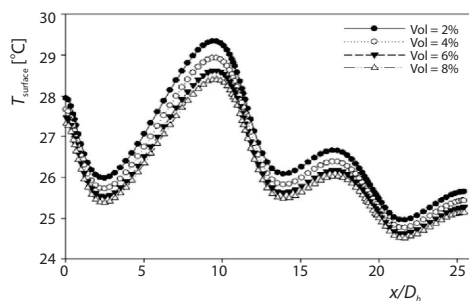


Figure 7. Temperature distributions on surface for different volume ratios

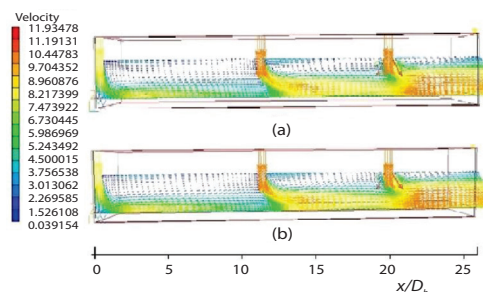


Figure 8. Velocity vectors for different volume ratio; (a)  $\varphi = 2\%$ , (b)  $\varphi = 8\%$

In impact region of the second jet, boundary-layer thickness is decreased and heat transfer increases. Highest temperature on the target plate was seen in second jet region. Because jet effect of second jet is decreased by the channel flow of first jet at wall jet region. Figure 9 shows temperature contours for CuO-water nanofluid with  $\phi = 2\%$  and  $8\%$ , respectively.

Effect of third jet reduces because of the channel flow of first and second jet. Jet effect and channel flow effect can also be seen at this region. Therefore, heat transfer rate has the highest level at this region. Figure 10 shows variation of local Nusselt number of fluids with different volume ratios. It can be seen that increasing volume ratio from  $\phi = 2\%$ - $8\%$  causes an increase of  $10.4\%$  on average Nusselt number. Average Nusselt number increases of  $4.3\%$  between  $\phi = 2\%$  and  $\phi = 4\%$ . This increase occurs  $7.7\%$  between  $\phi = 2\%$  and  $\phi = 6\%$ . So average Nusselt number increases while volume ratio is increased.

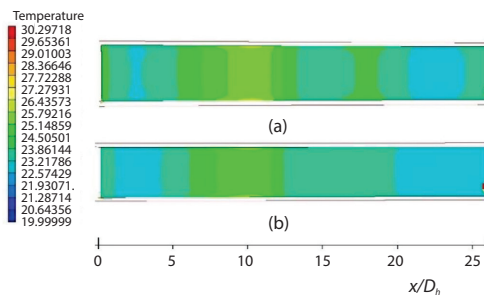


Figure 9. Temperature contours for different volume ratio (a)  $\phi = 2\%$ , (b)  $\phi = 8\%$

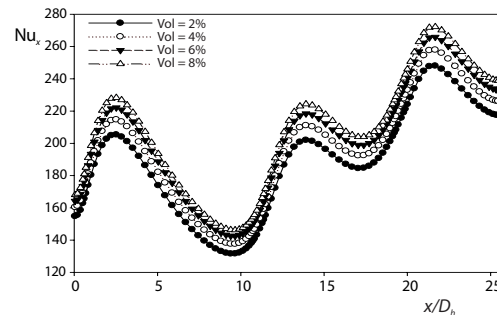


Figure 10. Local Nusselt numbers for different volume ratios

*Effects of heat flux of copper plate on heat transfer*

Figure 11 shows local Nusselt number for different heat flux ( $q'' = 37037 \text{ W/m}^2$ ,  $74074 \text{ W/m}^2$ ,  $148148 \text{ W/m}^2$ , and  $222222 \text{ W/m}^2$ ) with of copper surface when CuO-water nanofluid is used  $25 \text{ nm}$  particle size and  $\phi = 2\%$ . It can be seen that increasing heat flux on copper surface has not a considerable effect on local Nusselt number. Increasing heat flux six times has not a significant effect on average Nusselt number. Because of the jet effect of first jet local Nusselt number increases at the stagnation point of first jet.

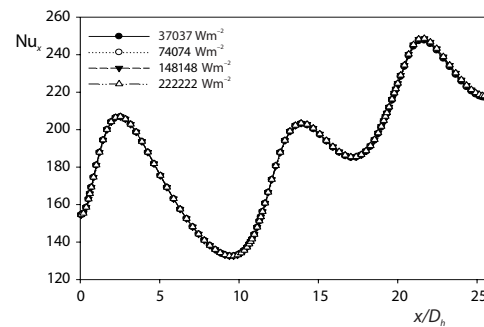


Figure 11. Local Nusselt numbers of nanofluid for different heat fluxes

Local Nusselt number decreases at the stagnation point of the seconde jet, because of the velocity decrease of nanofluids at this region. Local Nusselt number increases again at the region of third jet because jet effect and channel flow effect can be seen at this regiontogether.

*Effects of different types of nanofluid*

Numerical analysis is conducted for different type of nanofluid (Cu-water, CuO-water,  $\text{Al}_2\text{O}_3$ -water, and  $\text{TiO}$ -water, and pure water) with  $25 \text{ nm}$  particle size and  $\phi = 2\%$ . Properties of nanofluids were calculated at  $293 \text{ K}$ . Table 2 shows thermophysical properties of nanofluids (density, specific heat, kinematic viscosity, thermal conductivity, thermal expansion coefficient)

at 293 K. Local Nusselt numbers show that nanofluids with higher thermal conductivity cause higher heat transfer rate and higher local Nusselt number. For different types of nanofluids, difference between local Nusselt numbers is higher at the region of which nanofluid's velocity is higher than at the region of which nanofluid's velocity is lower.

**Table 2. Thermophysical properties of nanofluids at 293 K**

Nanofluid	Density, $\rho$ [kgm <sup>-3</sup> ]	Specific heat, $C_p$ [Jkg <sup>-1</sup> K <sup>-1</sup> ]	Kinematic viscosity, $\gamma$ [m <sup>2</sup> s <sup>-1</sup> ]	Thermal conductivity, $\lambda$ [Wm <sup>-1</sup> K <sup>-1</sup> ]	Thermal expansion coefficient $\beta$
Cu-water	1157.43	3594.13	0.000000902	0.6422	0.0001544
CuO-water	1108.23	3754.31	0.000000943	0.6391	0.0001540
TiO-water	1063.24	3902.51	0.000000982	0.6382	0.0001537
Al <sub>2</sub> O <sub>3</sub> -water	1055.84	3931.45	0.000000989	0.6378	0.0001534

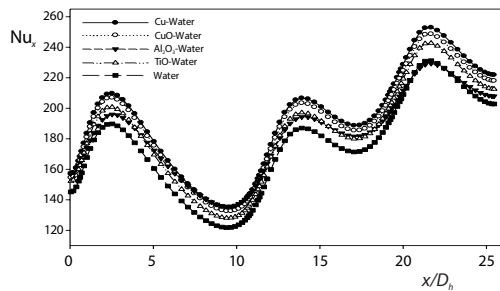


**Figure 12. Nusselt numbers for different type of nanofluids**

fluids shows better heat transfer performance. Nanoparticles in the base fluid increase the thermal conductivity of the base fluid.

## Conclusion

Present study is focused on numerical investigation of heat transfer and fluid-flow from a heated surface by using nanofluids and impinging jets. Effects of volume ratio, different heat flux and different types of nanofluids (Cu-water, CuO-water, Al<sub>2</sub>O<sub>3</sub>-water, TiO-water, and pure water) on heat transfer and fluid-flow were studied numerically. It is obtained that increasing volume ratio from  $\phi = 2\%$  to  $8\%$  causes an increase of  $10.4\%$  on average Nusselt number. Increasing heat flux six times has not a significant effect on average Nusselt number. Using using Cu-water nanofluid causes an increase of  $2.2\%$ ,  $5.1\%$ ,  $4.6\%$ , and  $9.6\%$  on average Nusselt number with respect to CuO-water, TiO-water, Al<sub>2</sub>O<sub>3</sub>-water, and pure water. Using Cu-water nanofluids shows the best heat transfer performance. Difference between numerical results and experimental results is less than  $5\%$  for this study. Research areas for future investigations can be using different particle diameter and different types of nanofluids with different application geometries.

## Acknowledgment

The financial support of this study by Scientific Research Project (16103021) of Adana Science and Technology University is gratefully acknowledged.

Figure 12 shows variation in Nusselt number for Cu-water, CuO-water, Al<sub>2</sub>O<sub>3</sub>-water, TiO-water nanofluids, and pure water. It was obtained that using Cu-water nanofluid causes an increase of  $2.2\%$ ,  $5.1\%$ ,  $4.6\%$ , and  $9.6\%$  on average Nusselt number with respect to CuO-water, TiO-water, Al<sub>2</sub>O<sub>3</sub>-water and pure water. It can be seen that using Cu-water nanofluid shows better heat transfer performance. The current numerical study shows that using nanofluids in spite of traditional heat transfer

## Nomenclature

$C_{p_{nf}}$  – nanofluid specific heat, [ $\text{Jkg}^{-1}\text{K}^{-1}$ ]  
 $C_{pp}$  – particle specific heat, [ $\text{Jkg}^{-1}\text{K}^{-1}$ ]  
 $D_h$  – hydrolic diameter, [mm]  
 $d_p$  – particle diameter, [nm]  
 $H$  – channel hight, [m]  
 $h_{avg}$  – average heat transfer convection coefficient, [ $\text{Wm}^{-2}\text{K}^{-1}$ ]  
 $k_{eff}$  – effective thermal conductivity, [ $\text{Wm}^{-1}\text{K}^{-1}$ ]  
 $k_{nf}$  – nanofluid thermal conductivity, [ $\text{Wm}^{-1}\text{K}^{-1}$ ]  
 $k_p$  – particle thermal conductivity, [ $\text{Wm}^{-1}\text{K}^{-1}$ ]  
 $Nu_x$  – local Nusselt number, ( $= QD_h/\Delta Tk_{nf}$ )  
 $Nu_{avg}$  – average Nusselt number, ( $= h_{avg}D_h/k_{nf}$ )  
 $Re$  – Reynolds number, ( $= V\rho D_h/\mu$ )

## Greek symbols

$\mu_{bf}$  – base fluid Dynamic viscosity, [ $\text{kgm}^{-1}\text{s}^{-1}$ ]  
 $\mu_{nf}$  – nanoparticle Dynamic viscosity, [ $\text{kgm}^{-1}\text{s}^{-1}$ ]  
 $\nu$  – kinematic viscosity, [ $\text{m}^2\text{s}^{-1}$ ]  
 $\rho_{bf}$  – base fluid density, [ $\text{kgm}^{-3}$ ]  
 $\rho_{nf}$  – nanofluid density, [ $\text{kgm}^{-3}$ ]  
 $\phi$  – the volume ratio of the suspended nanoparticles

## Subscript

bf – base fluid  
nf – nanofluid

## References

- [1] Kilic, M., et al., Experimental and Numerical Study of Heat Transfer from a Heated Flat Plate in a Rectangular Channel with an Impinging Jet, *Journal of the Brazilian Society of Mechanical Sciences and Engineering*, 39 (2017), 1, pp. 329-344
- [2] Kilic, M., Experimental and Numerical Study of Heat Transfer from a Heated Flat Plate in a Rectangular Channel with an Impinging Jet, Ph. D. thesis, Gazi University, Ankara, Turkey, 2013
- [3] Manca, O., et al., Thermal and Fluid Dynamics Behaviours of Confined Laminar Impinging Slot Jets with Nanofluids, *International Communications in Heat and Mass Transfer* 70 (2016), Jan., pp. 15-26
- [4] Lin, Z. H., et al., Heat Transfer Behaviours of a Confined Slot Jet Impingement, *International Journal of Heat and Mass Transfer*, 49 (1999), 5, pp. 2760-2780
- [5] McGuinn, A., et al., Surface Heat Transfer from an Impinging Synthetic Air Jet, *International Journal of Heat and Mass Transfer*, 20 (2005), Sept., pp. 1333-1338
- [6] Teamah, M. A., et al., Numerical and Experimental Investigation of Flow Structure and Behavior of Nanofluids Flow Impingement on Horizontal Flat Plate, *Experimental Thermal and Fluid Science*, 74 (2016), June, pp. 235-246
- [7] Sun, B., et al., Heat Transfer of Single Impinging jet with Cu Nanofluids, *Applied Thermal Engineering*, 102 (2016), June, pp. 701-707
- [8] Umar, A., et al., Experimental Study of Laminar Forced Convection Heat Transfer of Deionized Water Based Copper (I) Oxide Nanaofluids in Tube with Constant Wall Heat Flux, *Heat Mass Transfer*, 52 (2015), 10, pp. 2015-2025
- [9] Naphon, P., et al., Experimental Investigation of Titanium Nanofluids on the Heat Pipe Thermal Efficiency, *International Communication Heat and Mass Transfer*, 35 (2008), 10, pp. 1316-1319
- [10] Kilic, M., Ozcan, O., Numerical Investigation of Heat Transfer and Fluid-flow of Nanofluids with Impinging Jets, *Proceedings, International Conference on Advances And Innovations in Engineering*, Elazığ, Turkey, 2017, Vol. 1, pp. 434-440
- [11] Li, Q., et al., Experimental Investigation of Submerged Single Jet Impingement Using Cu-water Nanofluid, *Applied Thermal Engineering*, 36 (2012), 1, pp. 426-433
- [12] Xuan, Y., Li, Q., Investigation on Convective Heat Transfer and Flow Features of Nanofluids, *Trans. ASME J. Heat Transfer*, 125 (2003), 1, pp. 151-155.52
- [13] Corcione, M., Empirical Correlating Quations for Predicting the Effective Thermal Conductivity and Dynamic Viscosity of Nanofluids, *Energy Conversation Management*, 52 (2011), 1, pp. 789-793